Simplified Methodologies for Assessment and Design of Piles Affected by Lateral Spreading

Christopher R. McGann, **Ph.D. Student**
Pedro Arduino
Peter Mackenzie-Helnwein
University of Washington

Research Objectives

- Use numerical simulations to identify key factors which influence the behavior of piles embedded in laterally spreading soil during or after a seismic event.
- Establish simple analytic procedures which can be used by designers for the case of a pile subject to the lateral spreading load case.
- Increase the capabilities for 3D foundation modeling in the OpenSees finite element analysis platform.

3D Modeling Approach

[illegible] pressure-dependent strength

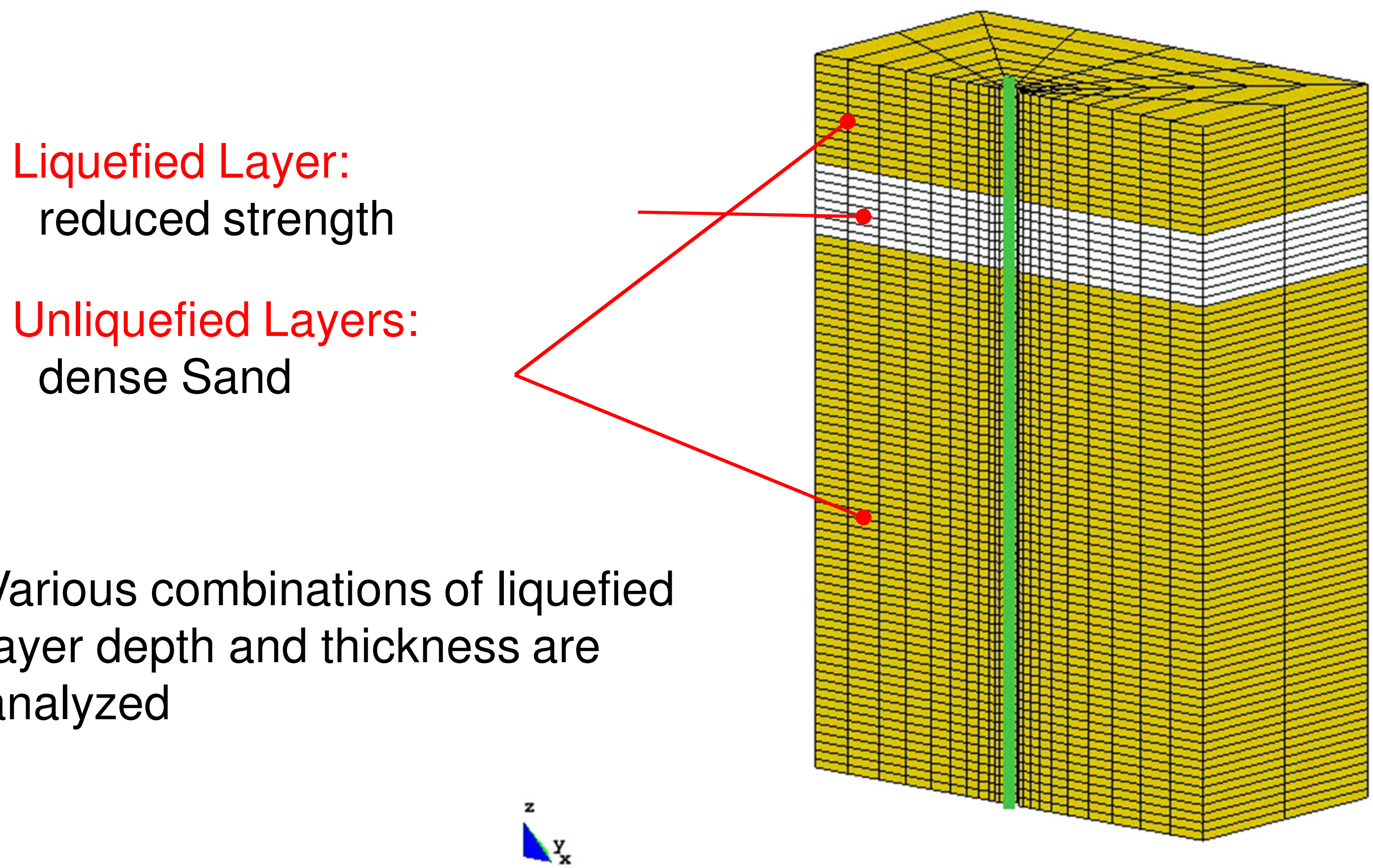

Various combinations of liquefied layer depth and thickness are analyzed

3D Modeling Approach

Beam-solid contact elements are used to model the soil-pile interface

The pile is modeled with beam-column elements

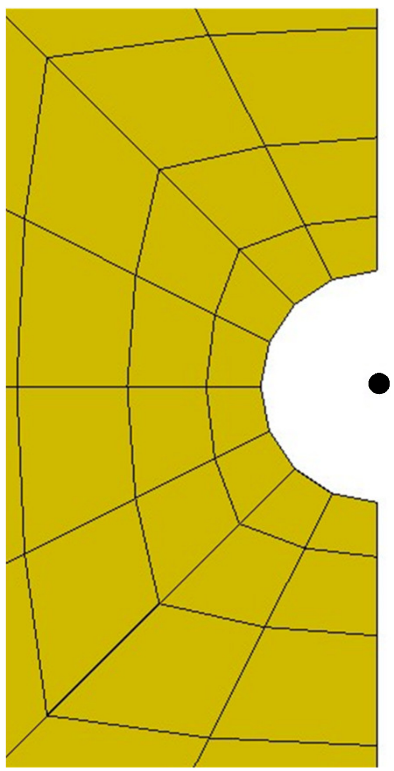

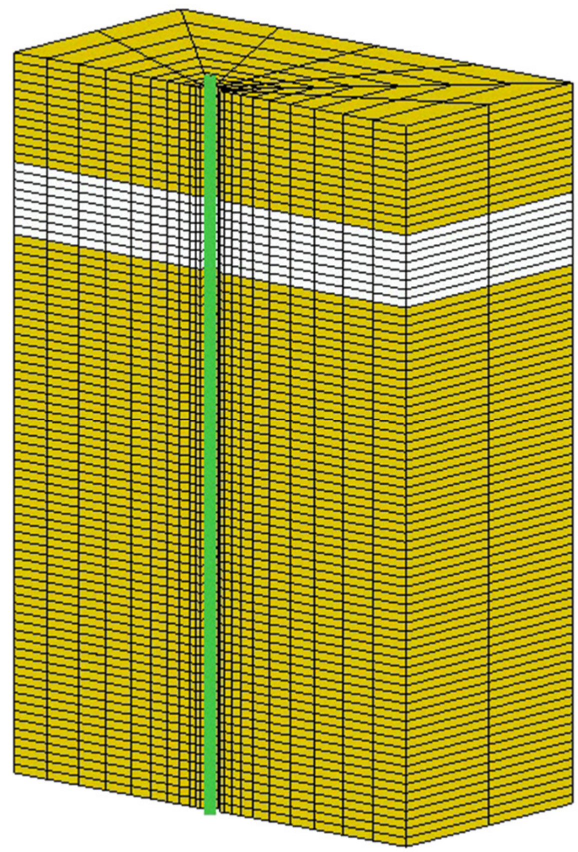

Three pile diameters are considered
(0.61, 1.37, 2.5 m)

3D Modeling Approach

Lateral spreading is modeled by applying a free-field displacement profile to the boundary of the model

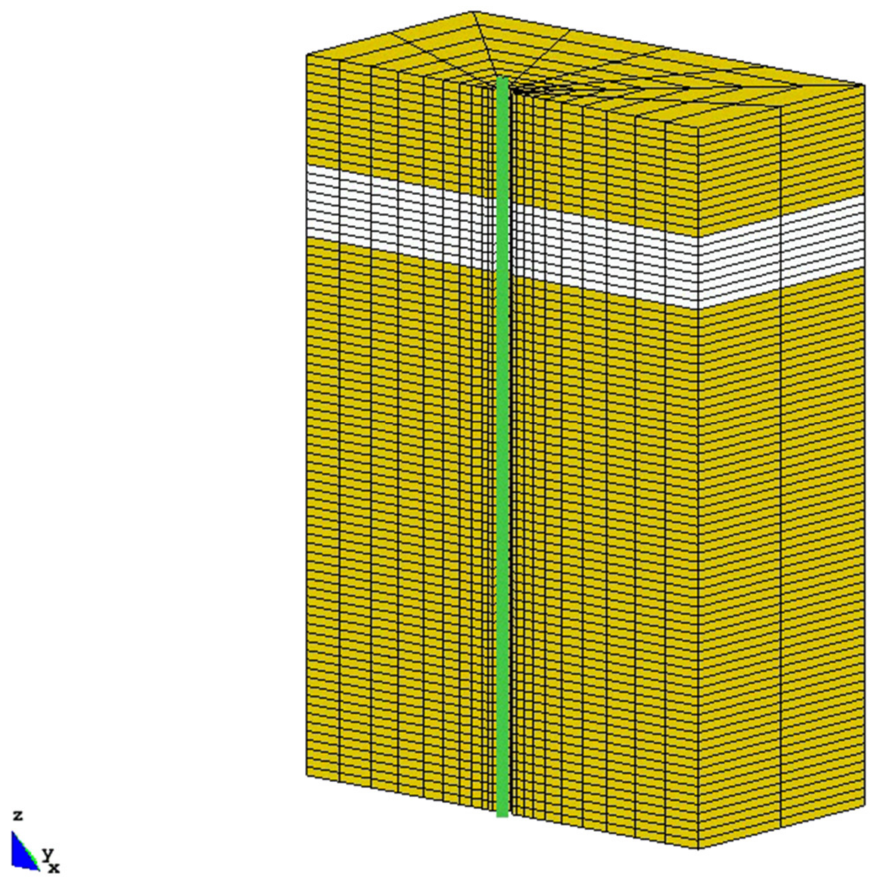

Beam-Solid Contact Elements

The beam-solid contact elements enable the use of standard beam-column elements for the pile

- This allows for simple recovery of the shear force and bending moment demands placed upon the pile
- Additionally, the surface traction acting on the pile-soil interface can be recovered and resolved into the forces applied by the soil to the pile

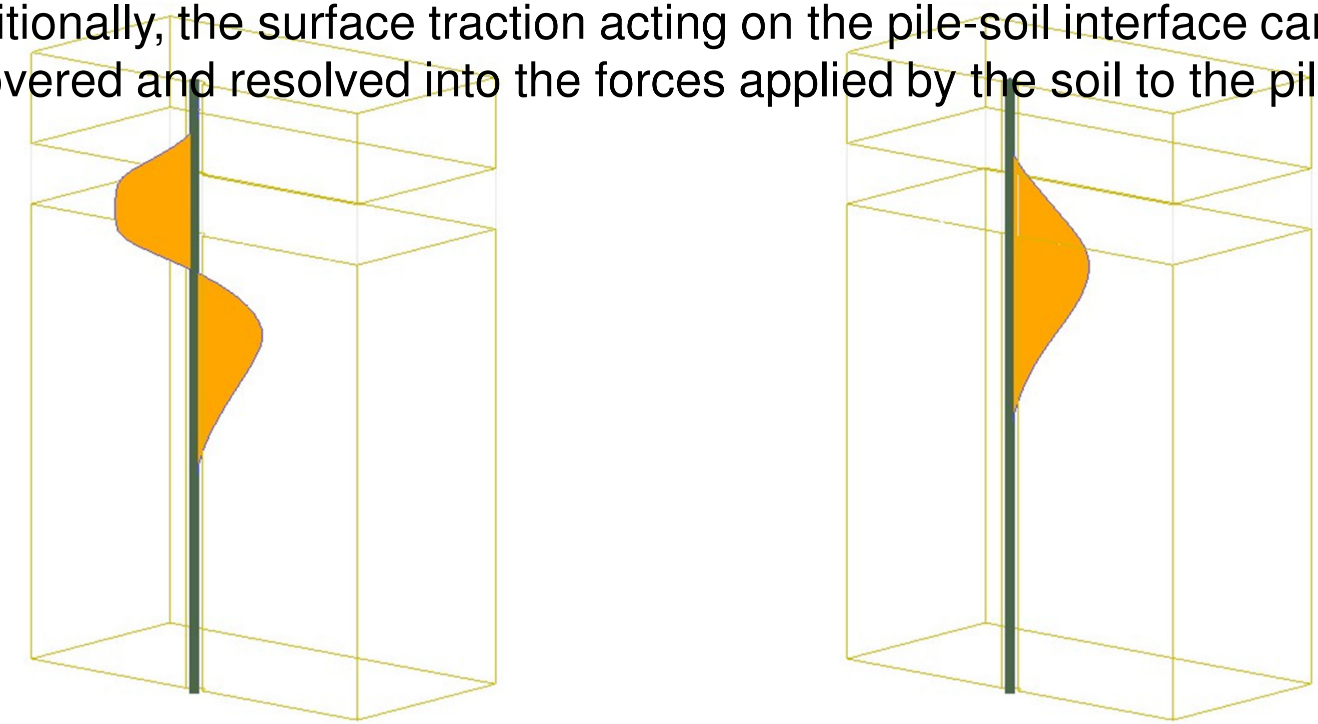

Computing *p-y* Curves: Rigid Kinematic

Work with 3D FE models has shown that use of a general pile deformation creates *p-y* curves which are influenced by the selected pile kinematics

A rigid pile kinematic is used to evenly activate the soil response with depth and to obtain *p-y* curves which are free from the influence of pile kinematics, reflecting only the response of the soil.

Computational process

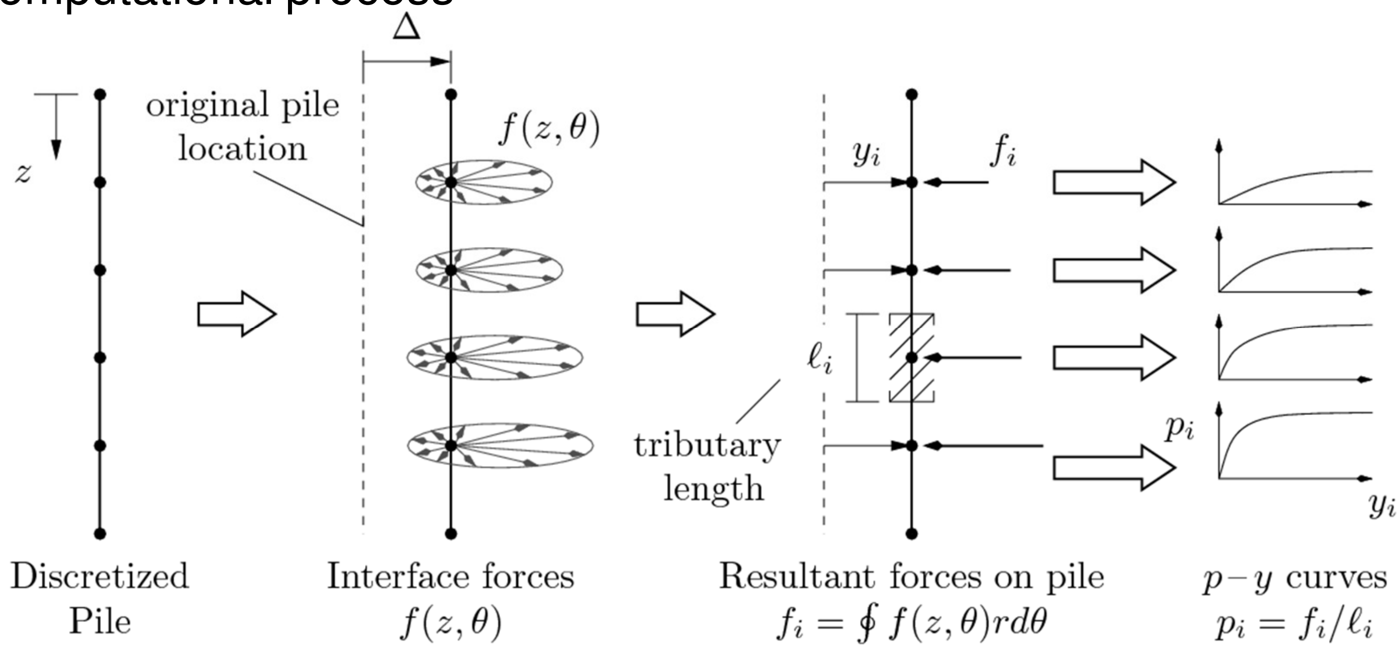

Computing *p-y* Curves: Parameters

The computed *p-y* curves are described by the function

$$p(y) = p_u \tanh\left(\frac{kz}{p_u} y\right)$$

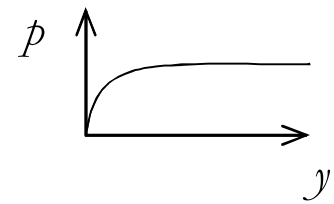

which is fit to the force-displacement data using least squares

Comparison and evaluation of the computed *p-y* curves is conducted using the two characteristic curve parameters

1. Initial stiffness, k_T

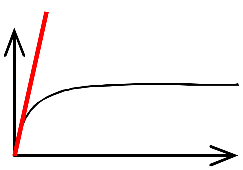

$$k_T = \left.\frac{dp(y)}{dy}\right|_{y=0} = kz$$

2. Ultimate resistance, p_u

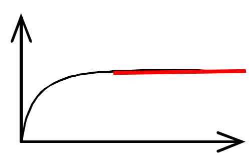

Initial Stiffness

A bilinear variation of initial stiffness is observed with increasing depth in the p-y curves computed using 3D FEA.

A linear variation of initial stiffness is proposed by the API. Here, the slope is matched to the FEA data to accentuate their difference.

The initial stiffness of the 3D FEA curves is similar to the API recommendations near the surface, but is significantly smaller at increased depths

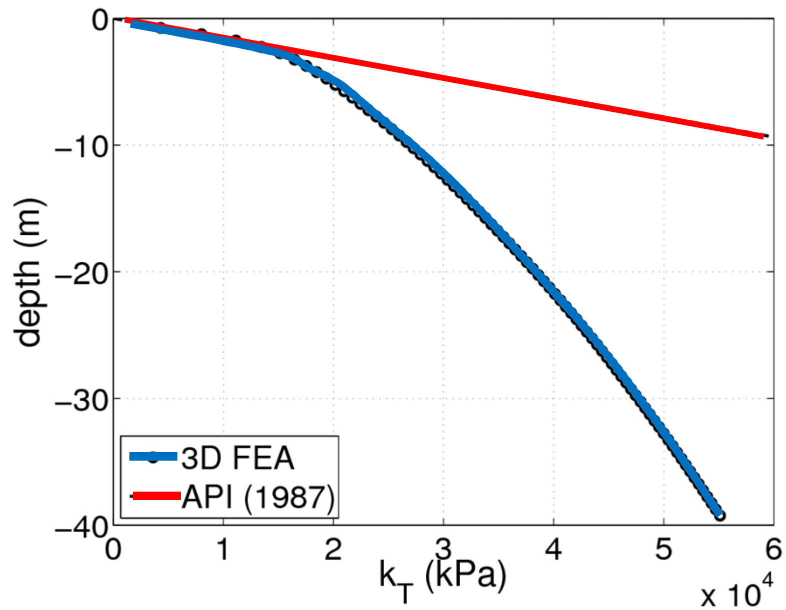

A parabolic distribution of initial stiffness, as used by Brandenberg et al. (2007) and Lam and Cheang (1995), or a similar bilinear distribution to that above is recommended for a static BNWF analysis of lateral spreading.

Ultimate Lateral Resistance

The distribution of ultimate lateral resistance with depth computed by the 3D FEA varies from distributions recommended by other researchers.

At shallow depths, all of the methods produce relatively similar results.

At increased depths, the 3D FEA values are much smaller than those recommended by the API.

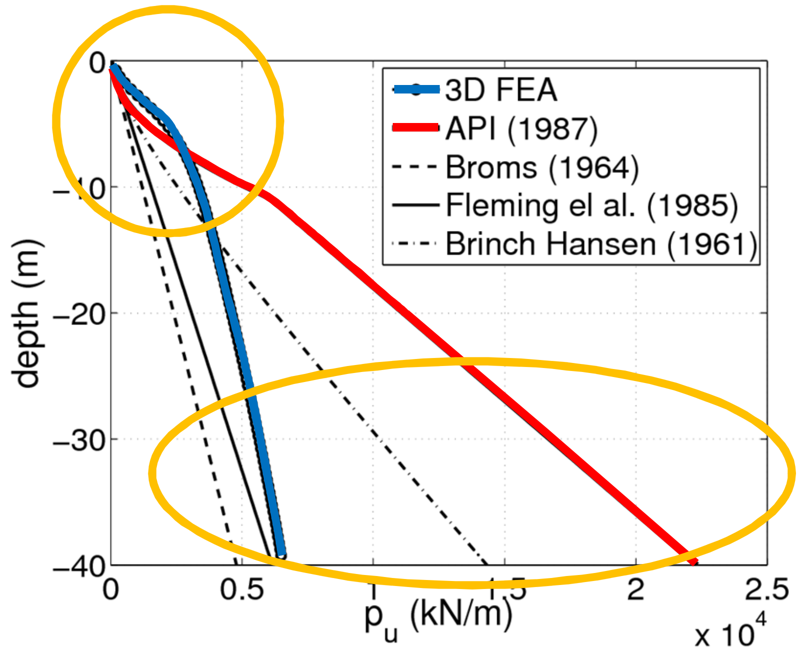

Use of one of the smaller distributions is recommended for *p-y* analyses of lateral spreading or other load cases in which deep soil-pile interaction is anticipated.

Influence of Liquefaction

The presence of the weaker liquefied layer effectively reduces the available resistance of the adjacent portions of the unliquefied soil

This is manifested in a reduction in the ultimate lateral resistance of the p-y curves near the liquefied layer

The initial stiffness of the unliquefied soil is also reduced, but the effect is more local to the liquefied interface

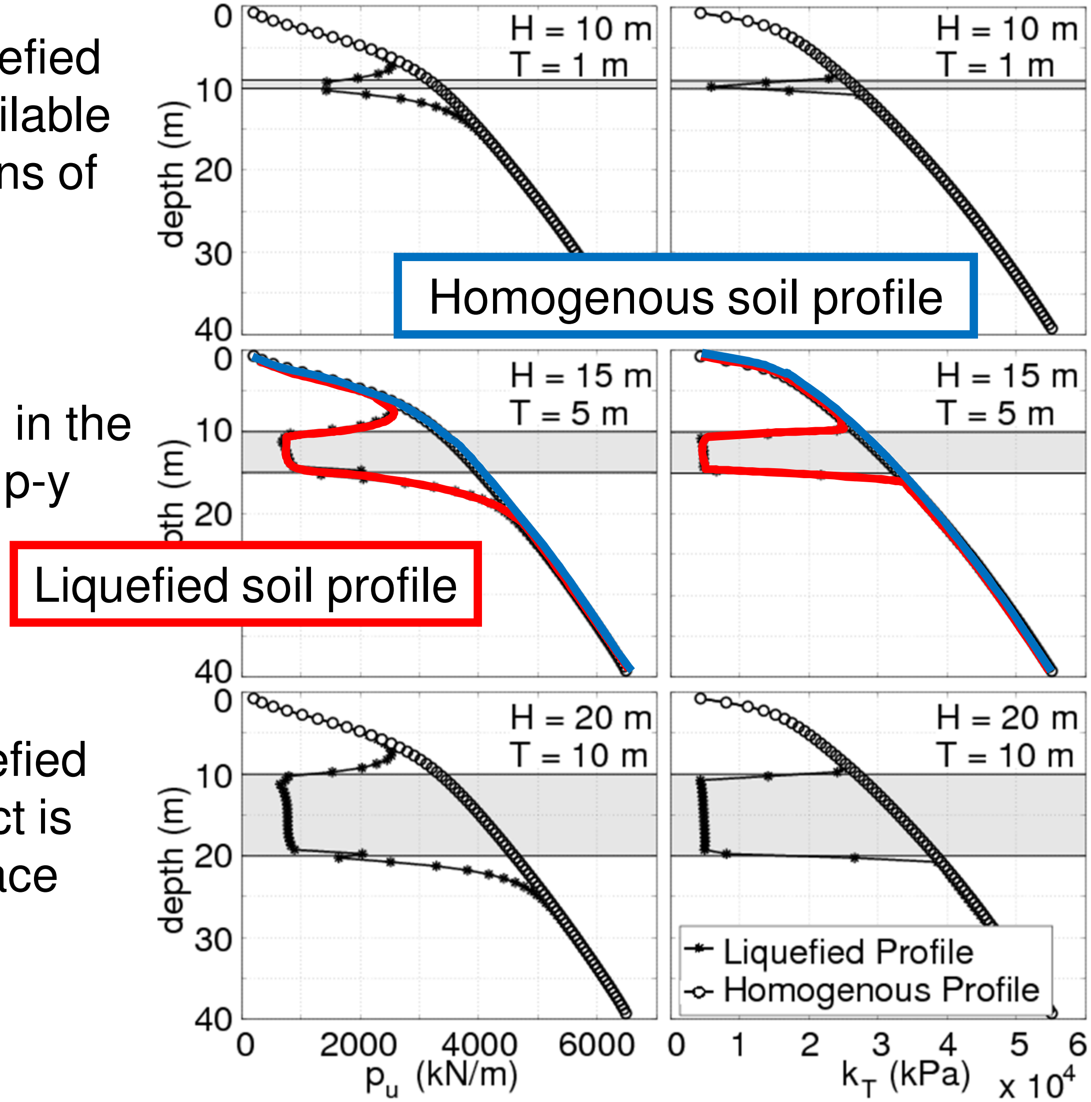

Development of Reduction Factors

Reduction Ratios

The reduction in lateral resistance can be seen more clearly by taking the ratio of the parameters in the liquefied case to those in the homogenous case

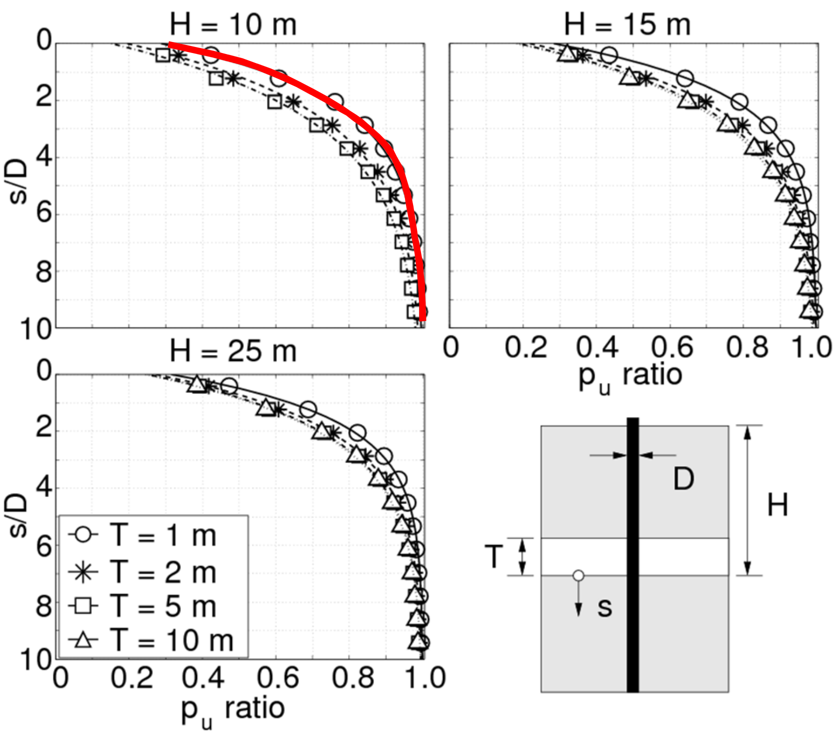

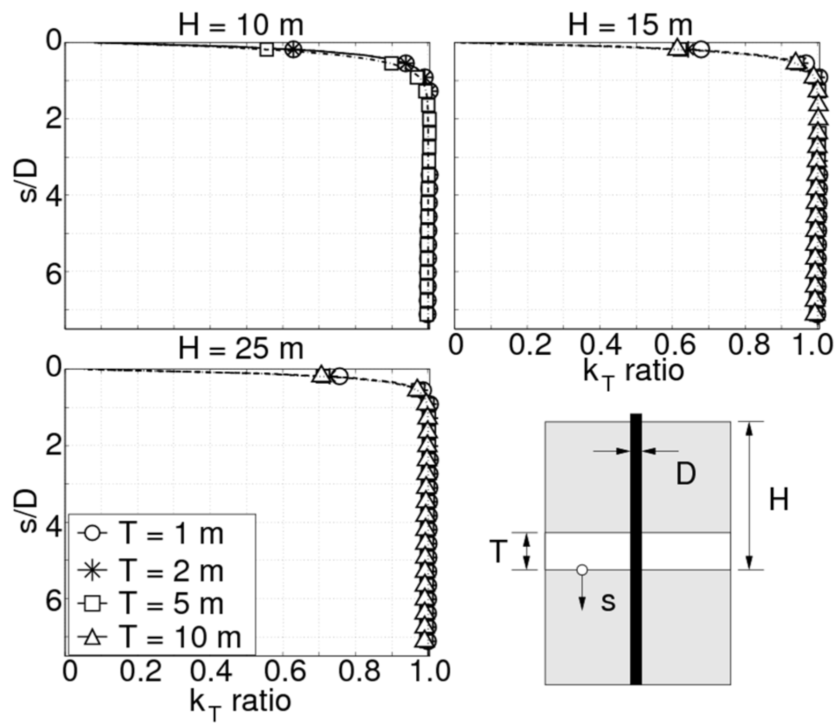

Reduction Ratios

The reduction in lateral resistance can be seen more clearly by taking the ratio of the parameters in the liquefied case to those in the homogenous case

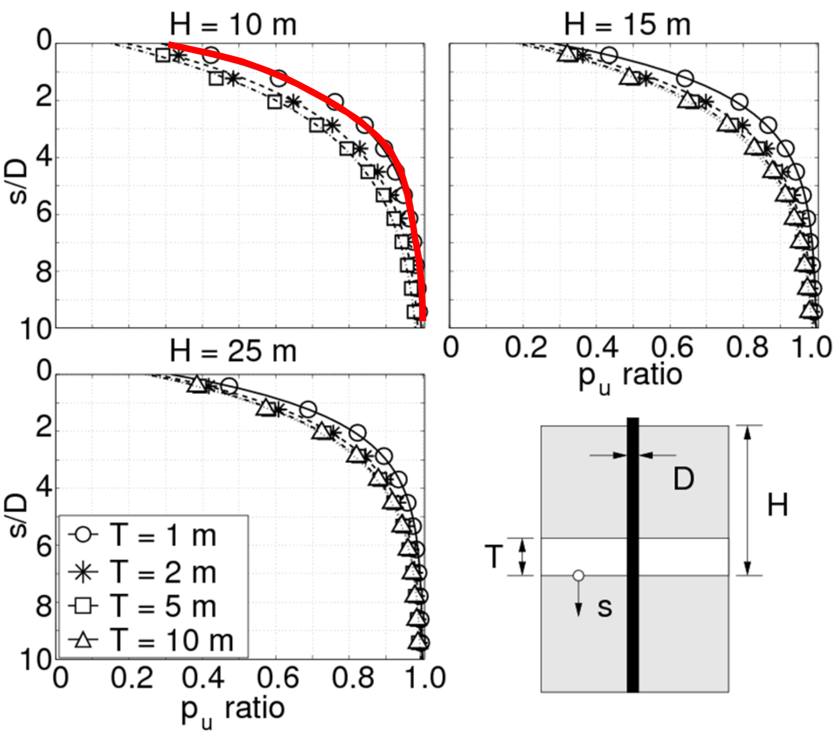

The observed reduction ratios suggest an exponential decay model

$$R^{(p,k)}(s) = 1 - R_0^{(p,k)} \exp\left(-\frac{s}{s_c^{(p,k)}}\right)$$

This model depends on two parameters

Interface reduction, $R_0^{(p,k)}$

Characteristic length, $s_c^{(p,k)}$

Parameter Identification

For each of three pile diameters, 21 soil profiles are used to compute the reductions in p-y curve parameters due to the presence of the liquefied layer

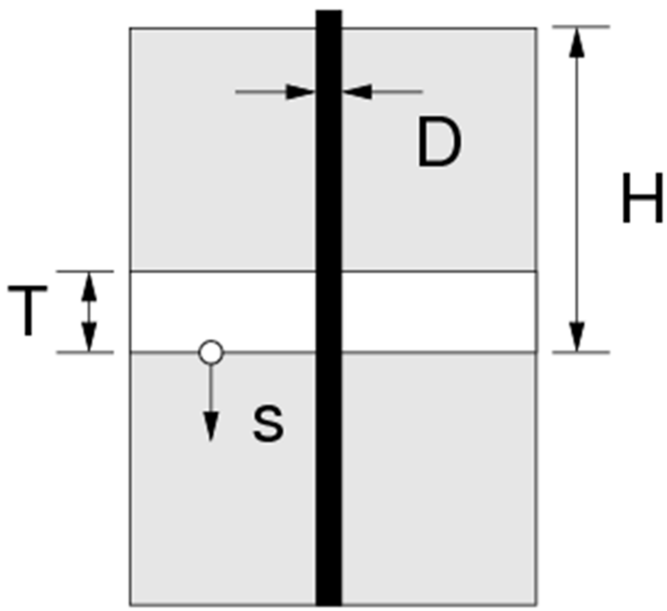

H (m)	T (m) 1	2	5	10
5	△	△		
10	▽	▽	▽	
11	◁			
12		◁		
15	○	○	○	○
16	▷			
17		▷		
20	◇	◇	◇	◇
25	□	□	□	□

Parameter Identification

Dimensionless parameters

$$\eta = R_0 \frac{\sigma'_v \tan\phi}{\gamma D} \qquad \xi = s_c \frac{\sigma'_v \tan\phi}{\gamma D^2} \qquad \beta = \frac{(\sigma'_v \tan\phi)^3 T}{\gamma^3 D^4}$$

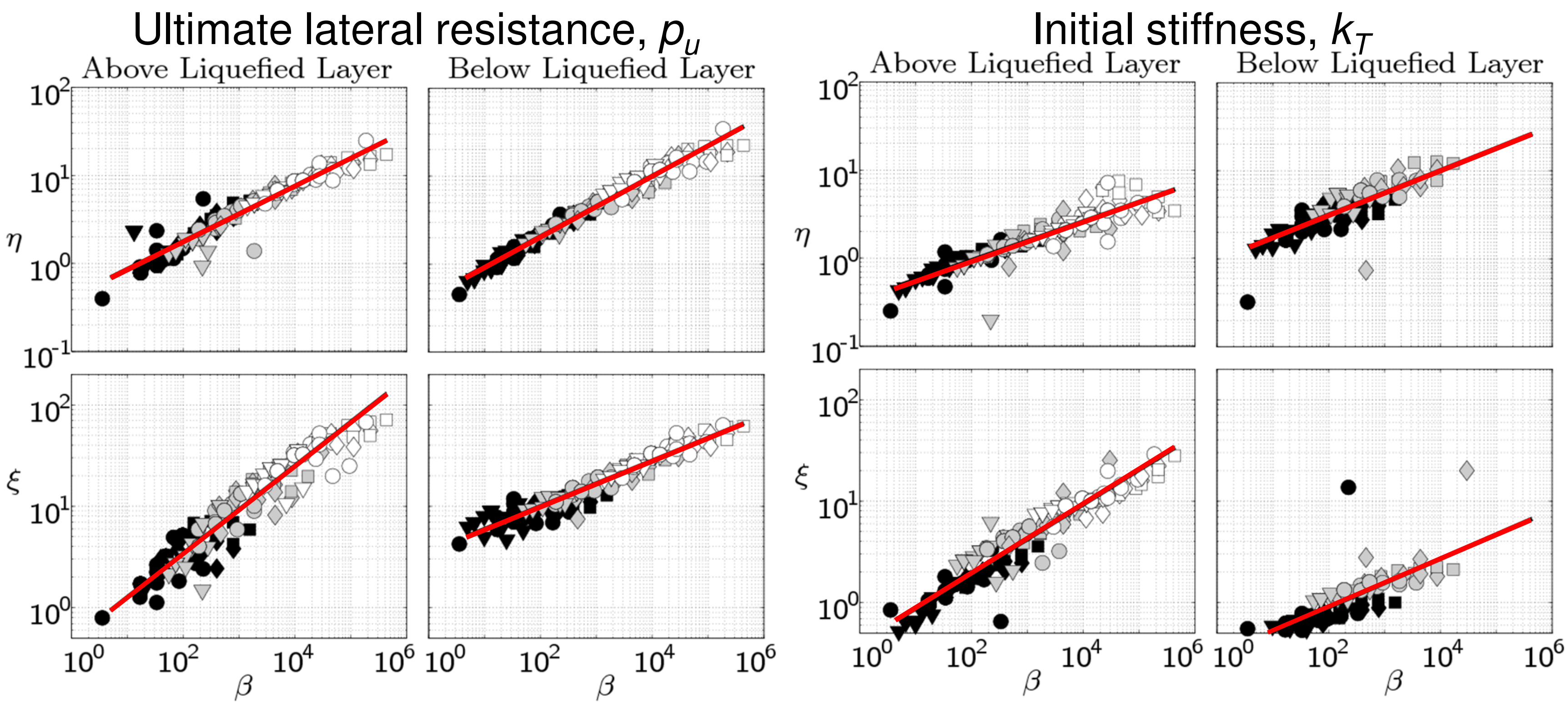

Parameter Identification

The lines of best fit can be used to compute the interface reduction and characteristic length for a particular soil profile

$$R_0^{(p,k)} = \frac{\gamma D}{\sigma_v' \tan\phi} a\beta^b$$

$$s_c^{(p,k)} = \frac{\gamma D^2}{\sigma_v' \tan\phi} c\beta^d$$

Ultimate lateral resistance, p_u

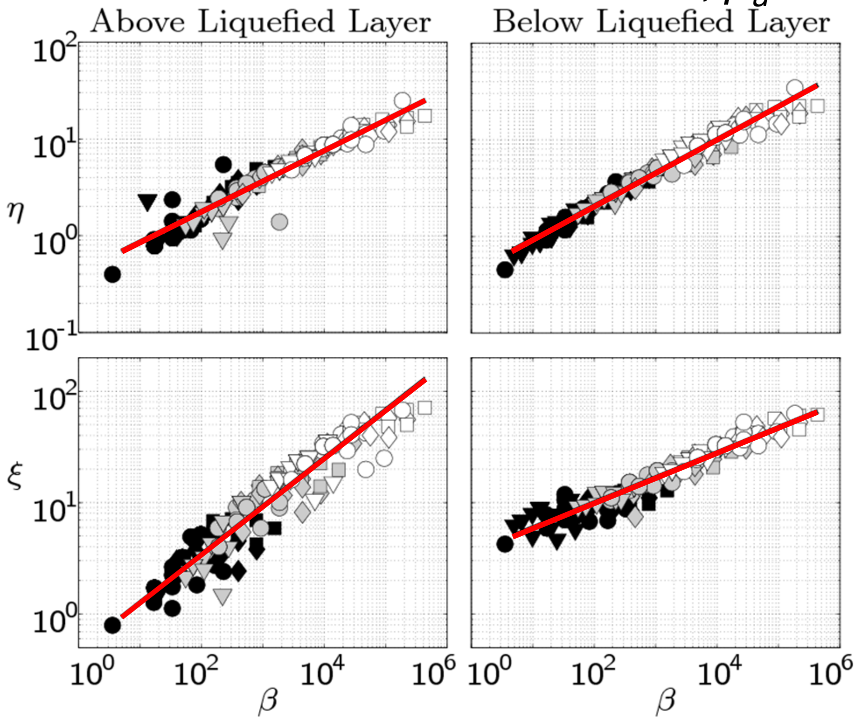

Initial stiffness, k_T

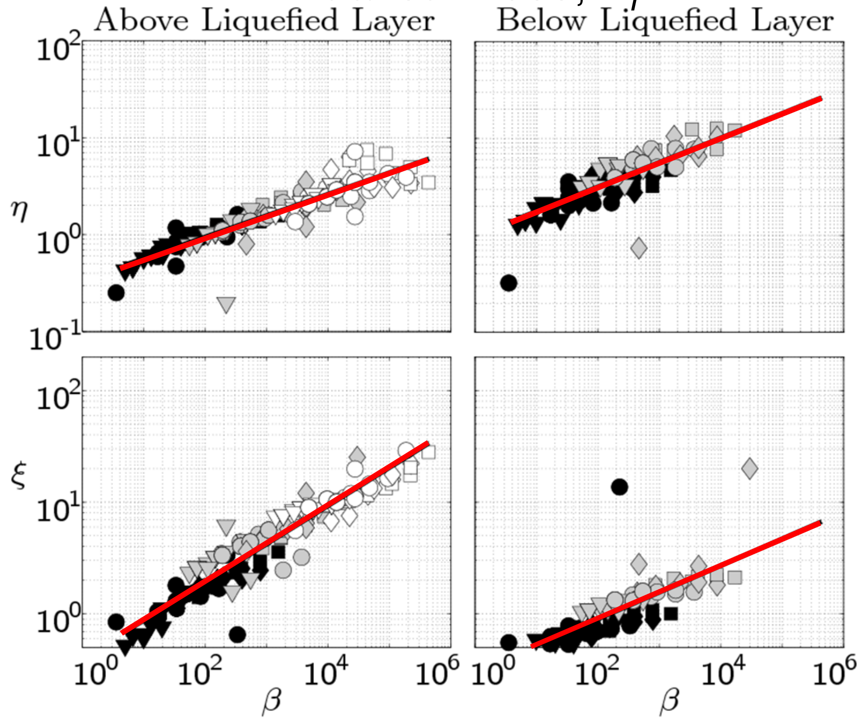

Computational Process

Reduction coefficients were computed which describe the best fit lines for the data set

Ultimate lateral resistance

	$R_0^{(p)}$		$s_c^{(p)}$	
	a	b	c	d
Above liquefied layer	0.421	0.315	0.474	0.432
Below liquefied layer	0.428	0.343	3.577	0.224

Initial stiffness

	$R_0^{(k)}$		$s_c^{(k)}$	
	a	b	c	d
Above liquefied layer	0.346	0.220	0.400	0.341
Below liquefied layer	1.000	0.252	0.299	0.239

Computational Process

These coefficients are used to compute the interface reduction and characteristic length

$$R_0^{(p,k)} = \frac{\gamma D}{\sigma'_v \tan\phi} a\beta^b$$

$$s_c^{(p,k)} = \frac{\gamma D^2}{\sigma'_v \tan\phi} c\beta^d$$

These parameters are used to compute reduction ratios using the exponential decay model

$$R^{(p,k)}(s) = 1 - R_0^{(p,k)} \exp\left(-\frac{s}{s_c^{(p,k)}}\right)$$

The reduced distributions of initial stiffness and ultimate lateral resistance are determined as functions of distance from liquefied layer through multiplication of the computed reduction ratios with any unreduced distribution

$$k_T^{(\text{reduced})}(s) = R^{(k)}(s) \cdot k_T^{(\text{unreduced})}(s)$$

$$p_u^{(\text{reduced})}(s) = R^{(p)}(s) \cdot p_u^{(\text{unreduced})}(s)$$

Development of Simplified Procedure

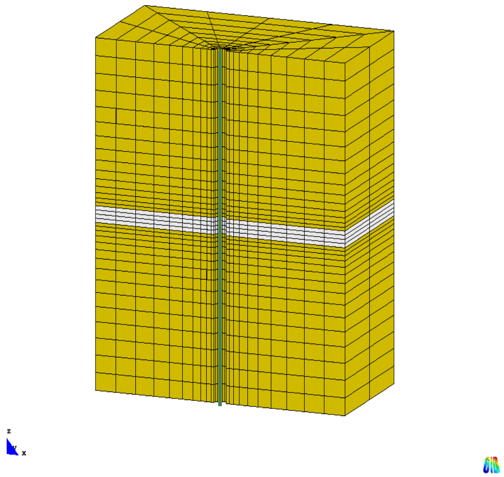

Perform 3D simulations

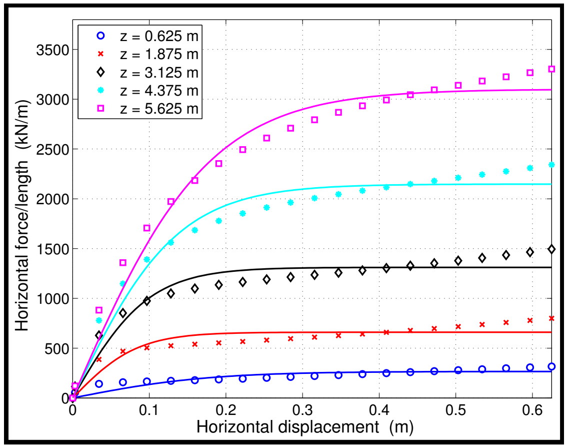

Extract *p-y* curves

Perform parametric analysis using 1-D mode

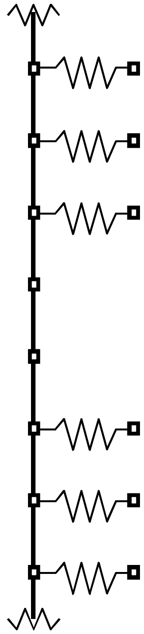

Development of Simplified Procedure

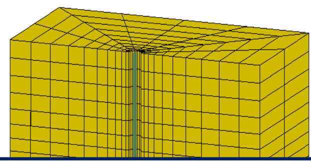

Parametric Analysis including:

- **Pile diameter D**
- **Pile stiffness EI**
- **Depth of liquefiable layer, H**
- **Thickness of liquefiable layer, T**
- **Soil friction angle, ϕ**
- **Soil unit weight, γ**

Perform parametric analysis using 1-D mode

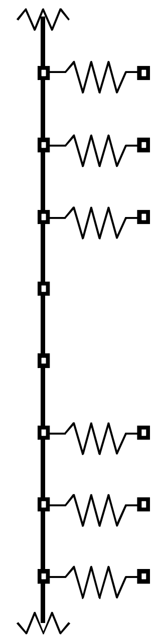

Effect of Soil displacement

Shear diagrams

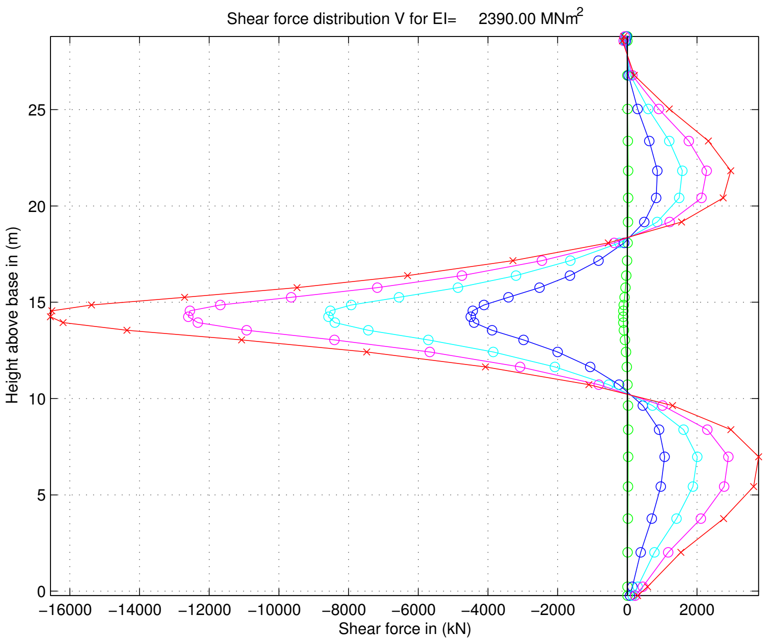

Bending Moment diagrams

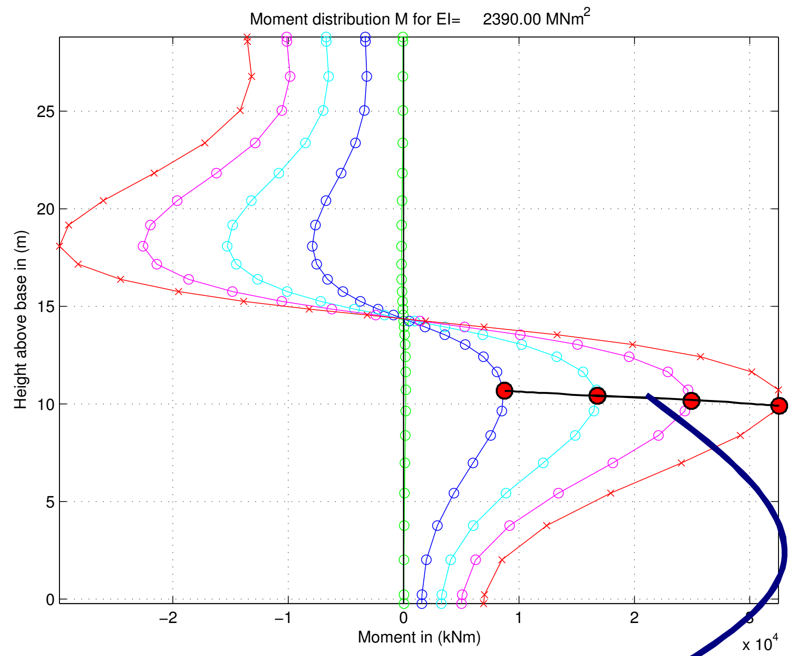

Location and value of maxV and maxM changes with soil displacement

Basic definitions

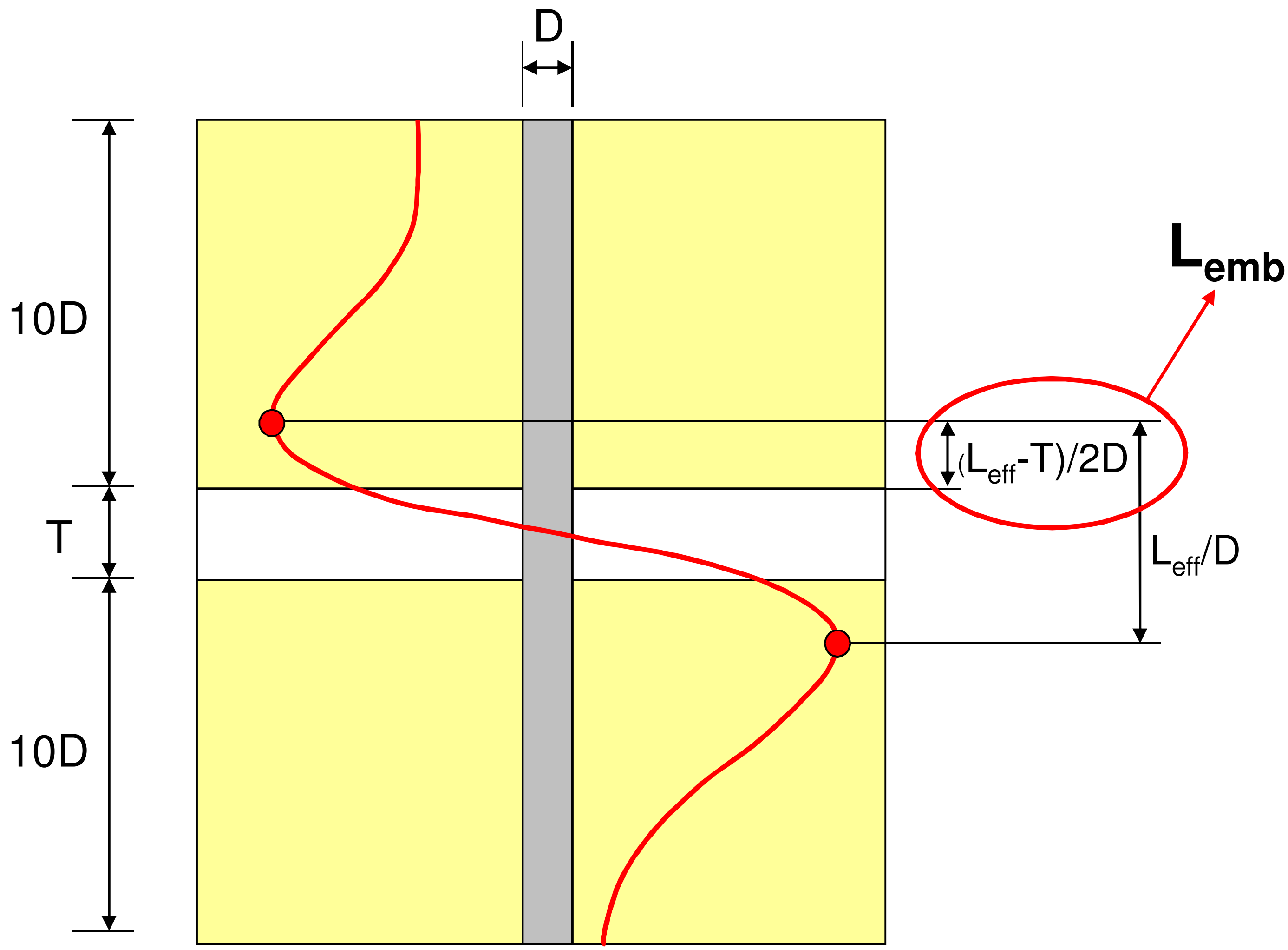

Non-dimensional characteristic parameter

$$\beta = \frac{\sigma'_v \tan\phi T^2 D^2}{EI}$$

- σ_v vert. effective stress at top of liq layer
- ϕ friction angle of non liq. Soil
- *EI* bending stiffness of the pile
- *T* thickness of the liquefiable layer
- *D* outer pile diameter

Embedment length in stiff soil layer (approximated as average of top and bottom layer)

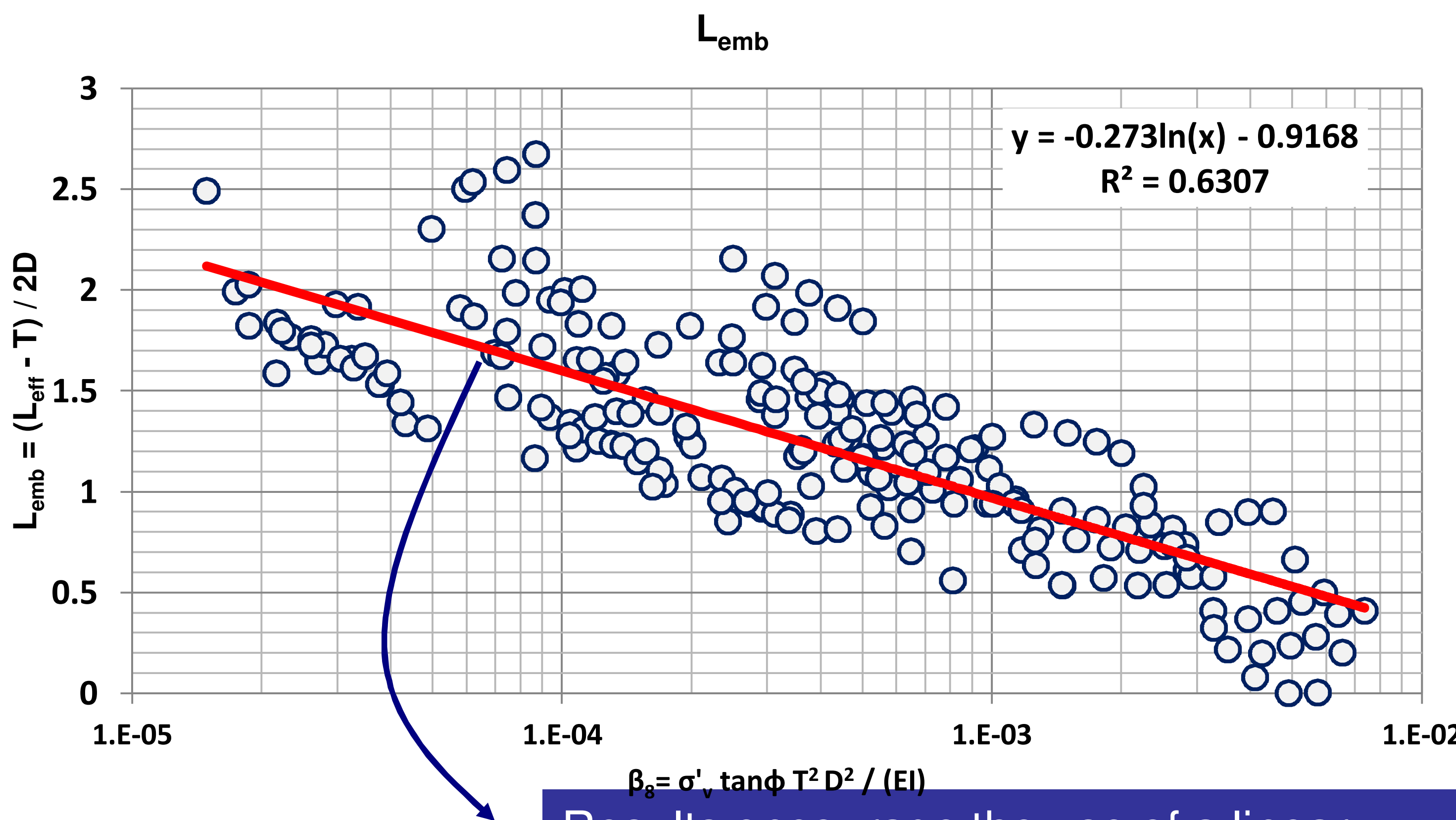

Results encourage the use of a linear regression for most of the parameter space

Dimensionless shear force demand

Maximum shear occurs within the liquefied layer.

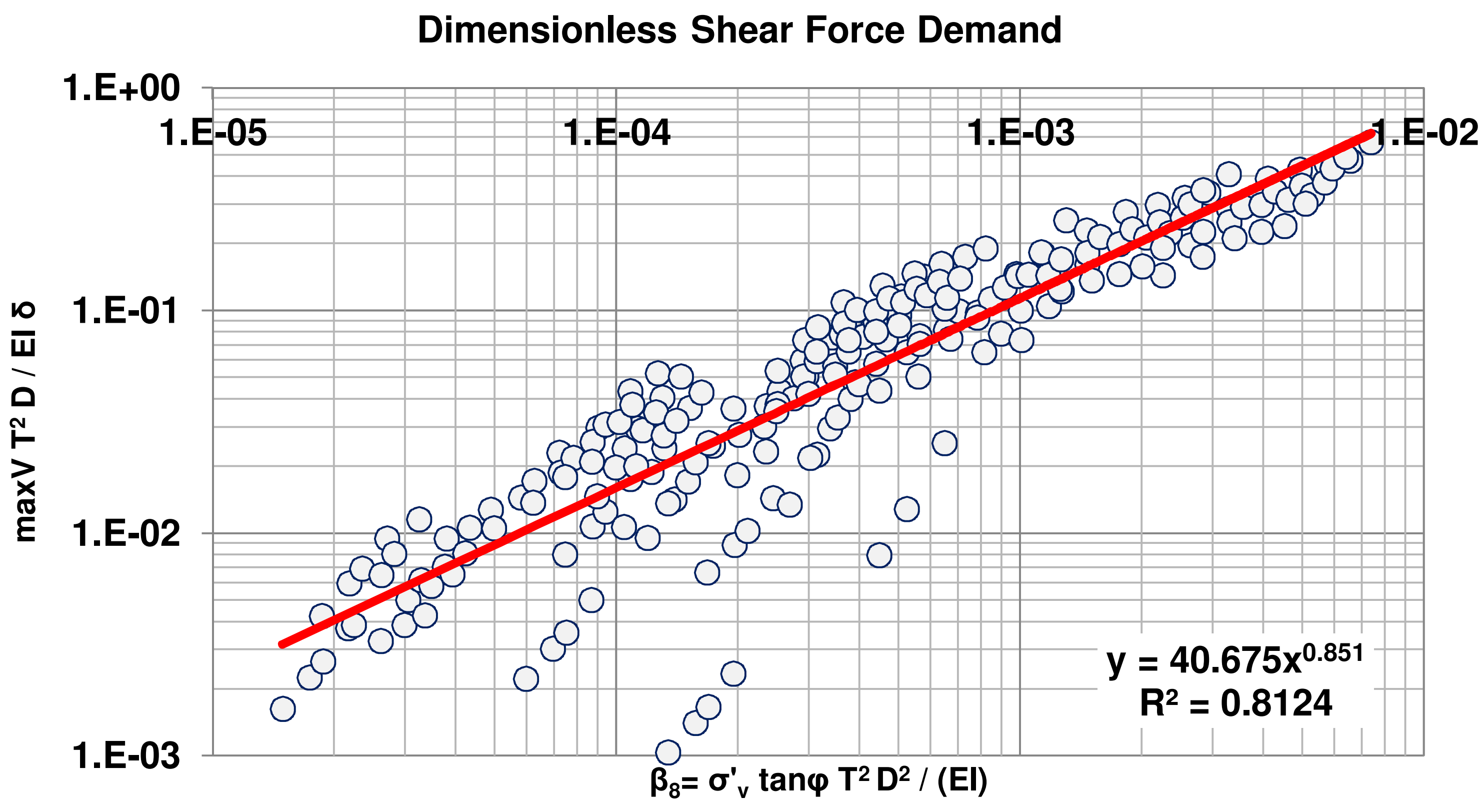

Dimensionless bending moment (or curvature demand).

Max M occurs at L_{embed} from the layer interface within the stiff layer

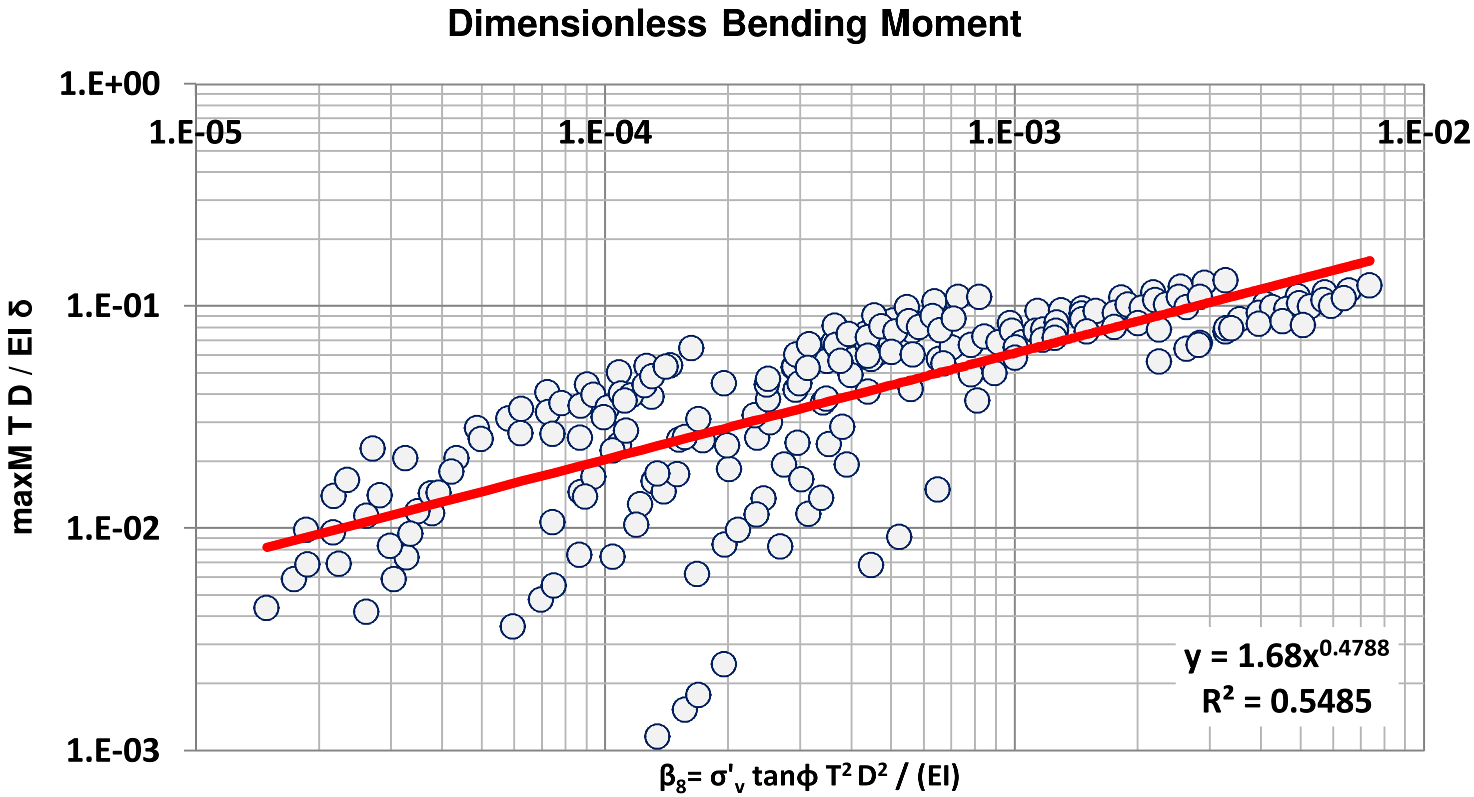

Design Procedure

$$\beta = \frac{\sigma'_v \tan\phi T^2 D^2}{EI}$$

→ Dimensionless characteristic parameter

$$\gamma_L = 1.2 - \log_{10}\beta$$

$$\gamma_V = 40.67\beta^{0.85}$$

$$\gamma_M = 1.68\beta^{0.47}$$

→ Non-dimensional coefficients

$$\max V = \gamma_V \frac{EI}{T^2}\frac{\Delta}{D}$$

→ Maximum shear force in the pile

$$\max M = \gamma_M \frac{EI}{T}\frac{\Delta}{D}$$

→ Maximum moment in the pile

$$L_{embed} = \gamma_L D$$

→ Location of maximum moment

Summary and Conclusions

- Representative *p-y* curves are computed from the 3D model using a rigid pile kinematic and it is found that the computed curves do not compare well with many conventionally-defined *p-y* curves.
- A reduction in the ultimate lateral resistance and initial stiffness of the *p-y* curves is observed in the unliquefied soil near the liquefied zone. The form of this reduction is well expressed by an exponential decay model.
- A parameter study was conducted to establish a means to predict reductions in the *p-y* curve parameters to account for the presence of a liquefied zone of soil.

- McGann, C. R., Arduino, P., and Mackenzie-Helnwein, P. (2010a). “Applicability of conventional p – y relations to the analysis of piles in laterally spreading soil.” *JGGE, ASCE, Under review.*
- McGann, C. R., Arduino, P., and Mackenzie-Helnwein, P. (2010b). “Simplified analysis procedure for piles in laterally spreading layered soil.” *JGGE, ASCE, Under review.*

Summary and Conclusions

- The proposed development of a simple though accurate design procedure may have important implications in current practice.
  - Fast, reliable and cost efficient design of pile foundations on sites subjected to lateral spreading.
  - Improve the understanding of the behavior of large diameter piles and thus may lead to changes in the current design practice which favors large numbers of small diameter piles.
- This project also demonstrates the benefits of 3D FEA over simplified models in applications where three-dimensional effects dominate.
- Proof of applicability of OpenSees as an advanced design tool.

Questions?